Available online at www.sciencedirect.com

ScienceDirect

Catalysis Today 137 (2008) 397–402

CATALYSIS TODAY

www.elsevier.com/locate/cattod

The influence of silver on the properties of cryptomelane type manganese oxides in N_2O decomposition reaction

Wojciech Gac [a,*], Grzegorz Giecko [a], Sylwia Pasieczna-Patkowska [a], Tadeusz Borowiecki [a], Leszek Kępiński [b]

[a] *Maria Curie-Skłodowska University, Faculty of Chemistry, Department of Chemical Technology, 3 Maria Curie-Skłodowska Square, 20-031 Lublin, Poland*

[b] *Institute of Low Temperature and Structure Research, PAS, Okolna 2, 55-422 Wrocław, Poland*

Received 25 July 2007; received in revised form 24 October 2007; accepted 8 November 2007

Abstract

The cryptomelane type oxides were prepared by the redox precipitation technique using $Mn(CH_3COO)_2$ and $KMnO_4$ precursors. Nitrogen sorption, XRD, TEM and TPD of oxygen studies showed changes of the surface, structural and redox properties of the samples upon silver introduction. Samples were investigated in the N_2O decomposition reaction. Direct introduction of silver to the synthesis mixture caused partial distortion of regular channel-like structure of the oxides, leading to the decrease of Mn–O bonds strength. As results samples showed slightly better catalytic activity at low temperatures, but were less stable at high temperatures. An introduction of silver by the impregnation method caused the decrease of the surface area of the samples, increase of surface oxygen mobility, leading to the small changes of activity.

Keywords: Manganese oxide; Silver; HREM; TPD; N_2O decomposition

1. Introduction

Nitrous oxide, N_2O is recently perceived as a relatively strong greenhouse gas with long atmospheric lifetime and large global warming potential [1,2]. N_2O participates in the depletion of stratospheric ozone. It is estimated, that about 60–70% of the total emission comes from anthropogenic contribution. The main source of N_2O emission is agriculture. The intensification of microbial nitrification, dentrification, and chemical processes, which occur in the soils, result from the agricultural activities, including an application of nitrogen synthetic fertilizers [3]. Strong impact on the N_2O emission shows wastewater sector. The major sources of N_2O emission are also the industrial processes, mainly nitric and adipic acids production, energy industry, manufacturing industries and transport. Therefore the reduction of emissions in the energy and chemical industry by the development of the production technologies, or the application of the catalytic abatement systems is an important target. The molecule of N_2O is thermodynamically unstable, and at high temperatures above 700 °C decomposes to nitrogen and oxygen. Nitrous oxide can be removed by chemical reaction with CO, H_2, C or NO. Direct catalytic decomposition of N_2O to N_2 and O_2 has been observed over large number of different types of catalysts, including noble metals, transition metal oxides, mixed oxides, spinels, perovskites, hydrotalcites, and zeolites [1,4]. The enhancement of the decomposition has been mainly attributed to the weakening the N–O bond. The first step of this process has been generally described as the adsorption of N_2O over active site, and then decomposition to N_2 and surface oxygen. Oxygen (O_2) is desorbed after surface reaction of two oxygen species or surface oxygen with N_2O molecule. The nature of the active sites has been widely discussed in the literature. High catalytic activity of iron- or cobalt-exchanged ZSM-5 catalysts has been attributed to the presence of isolated metal cations, which easily change their oxidation state during reaction cycle. The active sites in the supported or bulk oxide systems have been often related to the presence of coordinatively unsaturated surface transition metal ions.

Manganese oxides show large diversity of the structures and composition. The oxidation state of manganese in the oxides

---

* Corresponding author. Tel.: +48 81 5375526; fax: +48 81 5375565.
E-mail address: wojtek@hermes.umcs.lublin.pl (W. Gac).

0920-5861/$ – see front matter © 2007 Elsevier B.V. All rights reserved.
doi:10.1016/j.cattod.2007.11.008

varies from Mn^{2+} to Mn^{4+} depending on the preparation conditions, thermal treatment procedures and reaction conditions. Manganese oxide systems often play the role of oxygen storage, allowing transfer of oxygen between reacting molecules. The basic structural unit of manganese oxides is octahedron. The octahedra can be connected by the corners (e.g. in the perovskites), by the edges, leading to formation of the layered oxides, such as birnassite, or by the edges which form single, double, triple chains bounded by the corners, with hollandite, cryptomelane (2 × 2), romanechite (2 × 3), todorokite (3 × 3) type structures [5–7]. As results, one-dimensional square or rectangular channels are developed. Due to presence of small pores such materials can be used as molecular sieves for purification of water from heavy metal ions, e.g. As [8], Pb [9], Cd [10], Cr, Ni [11], separation of radionuclides [12–14], or as sorbents for light molecules. Recently tunnel structured oxides has been proposed by Becue as sulphur resistant adsorbents for NO_x [15]. He showed that nitrogen oxides could be adsorbed at low temperatures, and desorbed at high temperatures or removed in the air–fuel rich mixtures. Manganese oxides with the cryptomelane structure modified with silver have been demonstrated by King and Li as excellent SO_2 adsorbents for the Diesel vehicle applications [16]. Manganese oxides have been investigated in the catalytic decomposition of N_2O by several research groups [1,17–19]. High activity has been observed for Mn_2O_3 oxides. Obalová [18] and Tabata [19] related the activity of mixed manganese oxides to the coexistence of mixed manganese ions, partial substitution with Co and Al, or oxygen vacancies on the surface. We have shown that an introduction of silver to the perovskites or cryptomelane oxide systems increased the activity of the catalysts in the deep oxidation of methane and low-temperature CO oxidation reaction [20,21]. These effects have been ascribed to the increase of oxygen mobility and partial structural changes. The influence of silver on the activity of rhodium and palladium catalysts in the N_2O reduction has been recently observed by Tzitzios [22,23]. He attributed the increase of activity to the synergistic effects and weakening of metal–oxygen interactions.

The aim of the present work was to study the influence of silver on the microstructure, oxygen mobility and catalytic activity of cryptomelane manganese oxides in N_2O decomposition reaction.

2. Experimental

2.1. Catalyst preparation and characterization

Cryptomelane manganese oxides were prepared by the redox precipitation technique in the solution of acetic acid using the reaction between Mn^{2+} and MnO_4^{-} species and then refluxing in similar conditions to that described by Suib in [24]. In the first stage of typical synthesis 5.5 g of $Mn(CH_3COO)_2 \cdot 4H_2O$ was dissolved in 20 cm^3 of distilled water. Low pH of the solution was achieved by the introduction of 42 cm^3 of 6 wt.% acetic acid. Next 75 cm^3 of 4.1 wt.% solution of $KMnO_4$ was added dropwise while vigorous stirring. The mixture was refluxed at 50 °C while stirring for 24 h. The product was filtered, washed with 2 dm^3 of distilled water, and dried overnight at 80 °C. Finally the product was calcined at 250 °C for 2 h. Black crystalline material was obtained.

Silver was introduced by two different ways. The first series of catalysts (denoted Mn–Ag–R) were prepared by the direct addition of silver nitrate solution to the synthesis mixture before hydrothermal processing. Samples after refluxing were subjected to the same treatment conditions as pure manganese oxides. The second series of catalysts (denoted Mn–Ag–I) were prepared by the incipient wetness impregnation method. The obtained manganese oxides were impregnated with an aqueous solution of 0.5 M $AgNO_3$ under stirring. In order to obtain different silver loading the samples were impregnated several times with small portions of the solution with subsequent drying at 100 °C for 0.5 h and then final overnight drying. Samples were calcined at 250 °C for 2 h.

Catalysts composition was measured by applying the X-ray fluorescence method (ED-XRF Canbera 1510). The nitrogen adsorption/desorption isotherms were obtained volumetrically at $-196\,^{\circ}C$ using ASAP 2405N analyzer (Micromeritics Corp.). Samples were outgassed ($\sim 10^{-2}$ Pa) at 130 °C. The adsorption data were used to evaluate BET specific surface area (S_{BET}) and average pore diameter (D). X-ray diffraction studies (XRD) were done in the HZG-4 diffractometer using CuKα radiation ($\lambda = 1.5418$ Å). The microscopic studies have been done with transmission electron microscope Philips CM 20 SuperTwin with resolution 0.24 nm. Redox properties of the catalysts were investigated by the temperature-programmed desorption of oxygen (TPD). Studies were carried out in the AMI-1 system (Zeton Altamira). Samples were placed in the U-tube quartz reactor, and were initially heated in the mixture of 5% O_2/He (Praxair) with the total flow of 30 cm^3/min up to 250 °C (with the rate of 20 °C/min), then after 0.5 h were cooled down to room temperature. Desorption was conducted in He (Praxair) with the flow of 30 cm^3/min. The rate of the temperature increase was 10 °C/min. The evolved water was removed in a cold trap maintained in the LN_2–methanol mixture at $-98\,^{\circ}C$, placed between the reactor and thermal conductivity detector (TCD). Calibration of the TCD signal was performed by the injection of 55 μl O_2/He mixture to the He stream. The activity of catalysts in the N_2O decomposition reaction was studied using plug flow-quartz microreactor with inner diameter 10 mm. Samples (0.05 g) prior reaction were heated at 300 °C for 1 h using helium with a flow rate 100 cm^3/min. The flow rate of reaction mixture containing 1% N_2O in He was 100 cm^3/min. The reaction was studied in the range 300–750 °C. The experiments were conducted in the isothermal conditions for 30 min, with injections to gas chromatograph every 6 min. Analysis of reaction products was carried out, using a gas chromatograph Fisons GC8000, equipped with TCD detector and Porapak Q 100/120 mesh column.

3. Results and discussion

The applied preparation method allows obtaining manganese oxides with the cryptomelane structure, containing one dimensional 2 × 2 type channels with the size 0.46 nm × 0.46 nm

Table 1
Composition, surface area and mean pore diameter of the samples

Catalyst	Composition (wt.%)			S_{BET}(m^2/g)	D (nm)
	Mn	K	Ag		
Mn	58	5.6	–	217	11
Mn–Ag1–R	58	4.6	3.7	293	5.6
Mn–Ag2–R	56	2.4	10.3	277	7.7
Mn–Ag3–R	53	1.0	13.4	267	8.3
Mn–Ag4–R	50	<0.4	18.1	250	9.3
Mn–Ag1–I	54	5.8	3.2	160	15.5
Mn–Ag2–I	52	5.5	8.9	131	14.3
Mn–Ag3–I	49	5.8	15.3	128	14.7

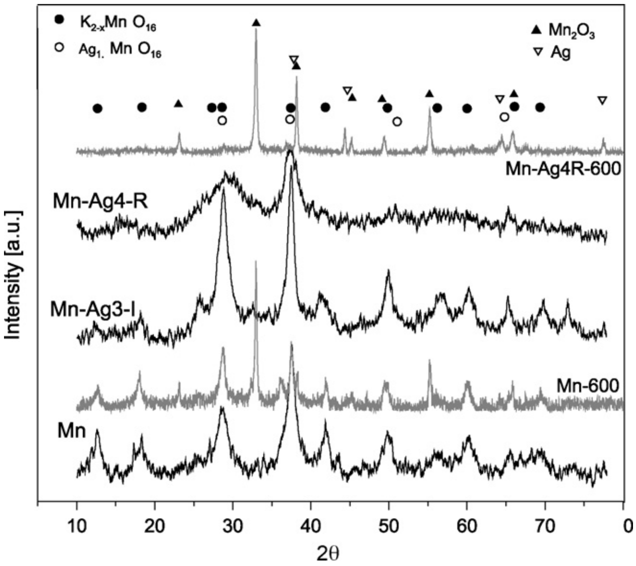

Fig. 1. XRD diagrams of the selected samples; grey curves samples calcined at 600 °C.

[21,24]. The surface area of unmodified manganese oxides is relatively large ($S = 217$ m^2/g) (see Table 1). An introduction of small amounts of silver by the direct addition to the synthesis mixture results in partial replacement of potassium ions from the channels. This process leads to the increase of the surface area of catalysts and formation of mesoporous structure [21]. However an increase of silver content causes the decrease of the surface area and increase of pore dimension (D). Smaller size of silver ions than potassium one, may induce changes of the structure of manganese oxide during their synthesis and thermal treatment, leading to the formation of the channels with different size, dislocations or oxygen vacancies. The distortion of the structure and the presence of silver ions or small silver crystallites can increase the number of active sites on the surface of manganese oxides and improve catalytic properties due to silver–manganese interactions. Potassium ions in the impregnation method are not subjected to the strong replacement processes. However an introduction of silver ions can change the surface properties of the oxide particles, resulting from the reduction of the number of free hydroxyl groups and deposition of strongly dispersed silver particles on the outer surface of the oxides.

Fig. 1 shows XRD curves for selected samples after calcination at 250 and 600 °C. The curves for unmodified and the impregnated manganese oxides well correspond to the cryptomelane phases of $K_{2-x}Mn_8O_{16}$ with the PDF No. 44-1386 of monoclinic crystalline structure with the *I2/m* space group, and PDF No. 42-1348 of tetragonal structure with the *I4/m* space group. An introduction of silver by the first method leads to the gradual decrease of ordered structure. Relatively small changes were recorded for selected reflections, e.g. located at the angles 28.7 and 37.5. The broad peaks and visible reflections for Mn–Ag4–R sample in the Fig. 1 may indicate the coexistence of partially distorted cryptomelane structures, manganese oxides on the different oxidation stages and silver containing species, including $Ag_{1.8}Mn_8O_{16}$ or $AgMnO_4$. The initial structure in the impregnated samples is preserved. Note, that XRD curves for both types of catalysts do not show clear reflections of silver metallic or oxide species. Thermal treatment of the samples at 600 °C leads to the partial decomposition of the initial structure and formation of Mn_2O_3 phase (PDF No.71-0636). An introduction of silver decreases thermal stability. Cryptomelane phase is hardly detected in the

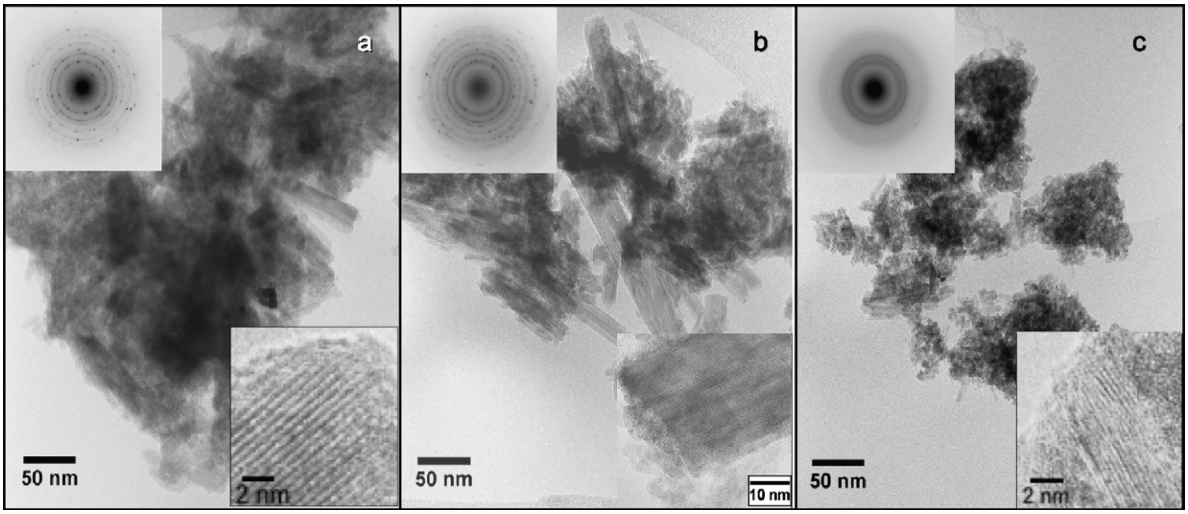

Fig. 2. TEM micrographs of the selected samples: (a) Mn; (b) Mn–Ag3–I; and (c) Mn–Ag4–R. Upper insets: SAED patterns; bottom insets: HRTEM images.

Mn–Ag4R sample, while Mn_2O_3 and silver reflections (PDF# 04-0783) are visible.

Fig. 2a illustrates the results of the transmission electron microscopy studies of the unmodified manganese oxides. Sample contains regular fibrous particles with the length ranging from 100 to 500 nm. Large number of the particles show rhomboidal cross-section with the side length 5–30 nm. Selected area electron diffraction (SAED) pattern taken from the large group of the particles contains sharp rings of $K_2Mn_8O_{16}$. The enlarged HRTEM image in the inset reveals the presence of parallel lattice fringes indicating high degree of crystal ordering. Similar needle-like nanoparticles can be found in the Mn-AgI-3 sample (Fig. 2b). However most of them are covered by the small irregular oxide species. For such species SAED pattern showed broad reflections, which confirmed the presence of the defects or dispersed oxide species. In turn, the morphology of the Mn–Ag4–R sample differs from that of Mn sample (Fig. 2c). Although the rings in the diffraction pattern are broad, their position still corresponds to the cryptomelane structure. HRTEM image (enlarged inset) reveals the presence of numerous crystal defects (cf. inset to Fig. 2a). Presented results confirm that direct introduction of silver to the synthesis mixture results partial decomposition of the manganese oxide structure. Sample consists of the small and more irregular particles with the size from 5 to 20 nm. Recently we have performed parallel studies of the samples by the FT-IR and FT-IR/PAS methods [25]. The characteristic feature of the FT-IR/PAS technique is that the signal is obtained from the suitable sampling depth, and relatively amplifies surface vibrations [26,27]. These studies confirmed structural changes of the samples caused by the direct introduction of silver to the synthesis mixture, and decrease of the number of hydroxyl groups in the impregnated samples. The discrepancies between the results obtained from these two techniques were attributed to more amorphous nature of the near-surface region of the samples due to different octahedra arrangement, various oxidation states of Mn, and the presence of surface hydroxyl groups.

The results of temperature programmed desorption of oxygen are shown in the Fig. 3. The course of oxygen removal depends on the amounts and the way of silver introduction. Weakly bounded oxygen (I) desorbs from the samples in the range 200–500 °C. The second stage for unmodified manganese oxides occurs in the range 500–700 °C (II), and in the next stage from 700 to 800 °C (III). The peak in the second stage is irregular, and indicates the presence of two types of oxygen species with similar Mn–O bond strength (IIa and IIb). An introduction of silver by the first method, gradually removes the most stable oxygen species, increases the number of IIa and IIb species, and enhances their desorption, i.e. leads to weakening of Mn–O bonds (Fig. 3a). In contrast, the impregnated samples show slight increase of the strength of Mn–O bonds of the II and III type oxide species with an increase of silver contents, and simultaneously the increase of weakly bounded oxygen (Fig. 3b). The later can be ascribed to desorption of oxygen from silver species. Suib and co-workers [28,29] assigned the peaks on the TPD curves of the tunnel-structured manganese oxides in the region 200–500 °C to the desorption of weakly chemisorbed oxygen and structural oxygen close to the surface, connected with lattice vacancies formation and often regarded as active sites in the oxidation reactions. While high temperature peaks they ascribed to the structural oxygen, responsible for stabilization of the structure of the oxides. We have recently shown that thermal treatment of the cryptomelane manganese oxides in the diluted oxygen below 500 °C led to slight increase of reducibility [21]. However the treatment at 600 °C removed easy reducible species and caused partial decomposition of the oxides, manifested by decrease of hydrogen consumption, and changes of the shape of reduction peaks. An introduction of silver strongly increased reducibility of the catalysts. The reduction processes began in hydrogen at

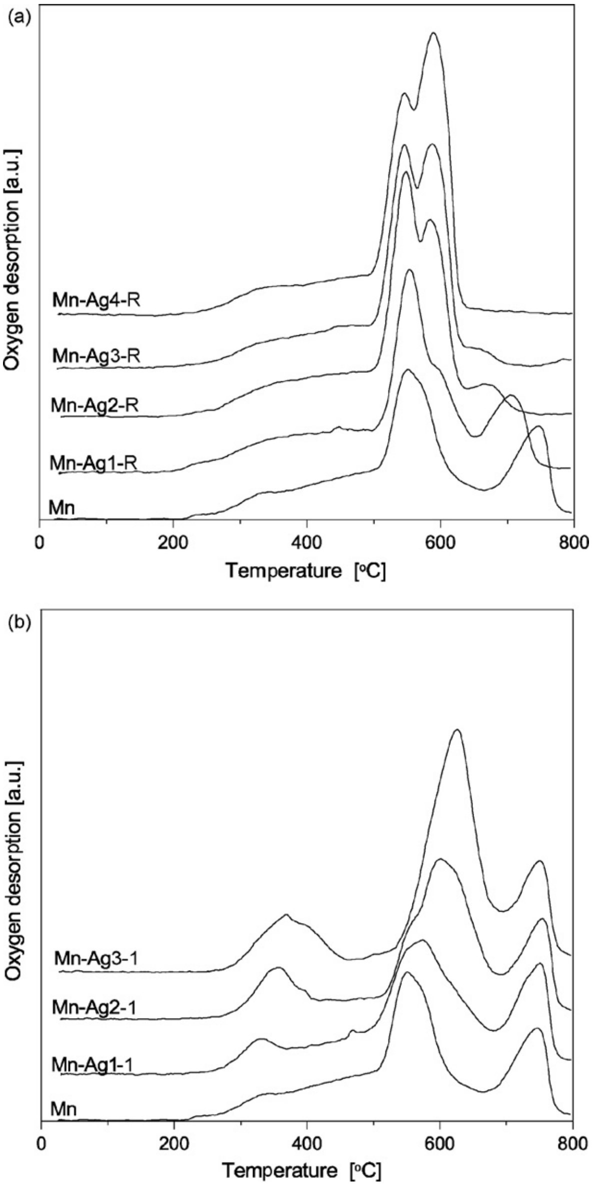

Fig. 3. (a) Temperature programmed desorption of oxygen from the first series of catalysts and (b) temperature programmed desorption of oxygen from the second series of catalysts.

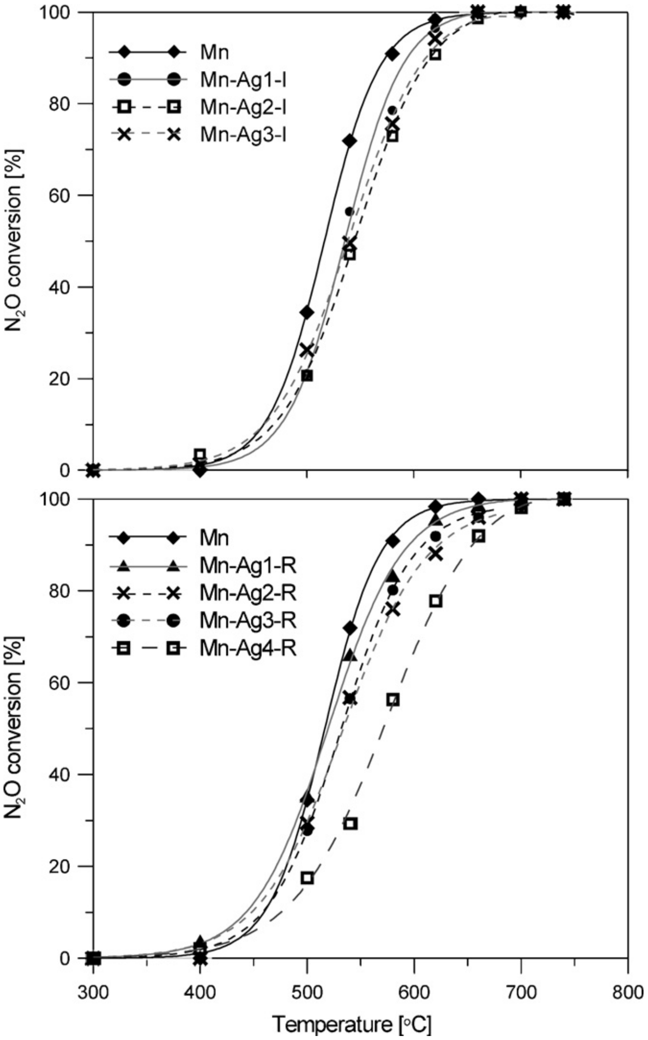

Fig. 4. N_2O conversion over silver modified manganese oxides.

room temperature, and at 200 °C were almost completed. However, high temperature treatment of these samples in the oxygen containing atmosphere led to the structural changes and strong decrease of reducibility.

Fig. 4 shows conversion curves of N_2O in the presence of two types of catalysts. Small conversion of N_2O can be observed for all catalysts below 400 °C; however complete conversion is recorded at around 650–700 °C. The presence of silver enhances to some extent the activity of catalysts at low temperatures. Slightly higher initial activity can be observed for Mn–Ag1–R catalysts. Although the catalysts contain relatively small amounts of silver, they show the largest surface area. In the series of impregnated catalysts high initial activity demonstrate silver rich catalysts. The enhancement can be explained by the increase of the number of active sites and high oxygen mobility caused by the introduction of silver. However all silver containing catalysts show worse activity at high temperatures. This effect increases with increase of silver contents. The differences between N_2O conversion over Mn and Mn–Ag4–R at the temperature of 600 °C approach 30%. The observed phenomena can be explained by the higher instability of structural oxygen. TPD and TPR studies of the first series of catalysts evidence that silver increases oxygen mobility at low temperatures, facilitates formation of oxygen vacancies or increases the number of manganese hydroxyl groups connected with manganese surface. When silver is deposited in the channels of manganese oxides, readily decreases the stability of the oxide structure. The decrease of activity at high temperature may by also connect with the changes of the nature of silver–oxygen interaction, and formation of more stable oxygen species. Such changes we have recently observed for small silver species confined in the channels of silica mesoporous materials and studied in the CO oxidation reaction [30].

The presented studies indicate that an introduction of silver to the cryptomelane manganese oxides can decrease their applicability for the processes which occur at high temperatures. It was widely discussed that decomposition of N_2O could occur at lower temperatures over different types of catalysts in the presence of oxygen ‘‘scavengers’’, such as carbon monoxide [31,32] or hydrocarbons [33,34]. The decrease of reaction temperature connected with addition of gaseous reductants can be beneficial for catalytic performance of the modified silver manganese oxides in N_2O decomposition reaction, and will be the subject of our future work.

4. Conclusions

Two types of silver modified cryptomelane manganese oxides were studied. The changes of the structural and surface properties were evidenced by the nitrogen adsorption/desorption, X-ray diffraction and transmission electron microscopy studies. Direct introduction of silver to the synthesis mixture caused partial distortion of regular channel-like structure of the oxides, leading to the decrease of Mn–O bonds strength. As the result the samples were less stable at high temperatures. An introduction of silver by the impregnation method caused the decrease of the surface area of the samples, and increased surface oxygen mobility. An introduction of silver slightly increased the activity of manganese oxides at low temperatures. However the modified oxides showed worse activity at high temperatures due to lower thermal stability.

Acknowledgement

This work was supported by the Polish Ministry of Education and Science as research project No. 3T09B11429.

References

[1] F. Kaptejin, J. Rodriguez-Mirasol, J. Moulijn, Appl. Catal. B Environ. 9 (1996) 25.
[2] J. Perez-Ramirez, Appl. Catal. B Environ. 70 (2007) 31.
[3] J. Zou, Y. Huang, Y. Lu, X. Zheng, Y. Wang, Atmos. Environ. 39 (2005) 4755.
[4] Y.F. Chang, J.G. McCarty, E.D. Wachsman, V.L. Wong, Appl. Catal. B Environ. 4 (1994) 283.
[5] Q. Feng, H. Kanoh, K. Ooi, J. Mater. Chem. 9 (1999) 319.
[6] J.E. Post, Proc. Natl. Acad. Sci. U.S.A. 96 (1999) 3447.

[7] S.L. Brock, N. Duan, Z.R. Tian, O. Giraldo, H. Zhou, S.L. Suib, Chem. Mater. 10 (1998) 2619.

[8] E. Deschamps, V.S. Ciminelli, W.H. Holl, Water Res. 39 (2005) 5212.

[9] M. Tsuji, Solvent Extract. Ion. Exch. 19 (2001) 531.

[10] S.R. Randall, D.M. Sherman, K.V. Ragnarsdottir, Chem. Geol. 151 (1998) 95.

[11] K. Tiede, T. Neumann, D. Stueben, J. Soils Sediments 7 (2007) 53.

[12] A. Dyer, M. Pillinger, J. Newton, R. Harjula, T. Möller, S. Aminet, Chem. Mater. 12 (2000) 3798.

[13] C. Guy, F. Audubert, J.E. Lartigue, C. Latrille, T. Advocat, C. Fillet, C. R. Phys. 3 (2002) 827.

[14] A. Bilewicz, B. Bartoś, R. Misiak, B. Petelenz, J. Radioanal. Nucl. Chem. 268 (2006) 485.

[15] T. Becue, G. Babilon, P. Villered, US Patent 679,724,7B2.

[16] L. Li, D.L. King, Ind. Eng. Chem. Res. 44 (2005) 7388.

[17] T. Yamashita, A. Vannice, J. Catal. 161 (1996) 254.

[18] L. Obalová, K. Pacultová, J. Balabánová, K. Jirátová, Z. Bastl, M. Valásková, Z. Lacny, F. Kovanda, Catal. Today 119 (2007) 233.

[19] K. Tabata, T. Karasuda, E. Suzuki, H. Taguchi, J. Mater. Sci. 35 (2000) 4031.

[20] A. Machocki, T. Ioannides, B. Stasinska, W. Gac, G. Avgouropoulosb, D. Delimaris, W. Grzegorczyk, S. Pasieczna, J. Catal. 227 (2004) 282.

[21] W. Gac, Appl. Catal. B Environ. 75 (2007) 107.

[22] T.N. Angelidis, V. Tzitios, Appl. Catal. B Environ. 41 (2003) 357.

[23] V.K. Tzitzios, V. Georgakilas, Chemosphere 59 (2005) 887.

[24] J. Luo, Q. Zhang, A. Huang, S.L. Suib, Micropor. Mesopor. Mater. 35/36 (2000) 209.

[25] W. Gac, J. Phys. IV 137 (2006) 283.

[26] D.W. Vidrine, Photoacoustic Fourier transform infrared spectroscopy of solids and liquids, in: J.R. Ferraro, L.J. Basile (Eds.), Fourier Transform Infrared Spectroscopy, vol. 3, Academic Press, New York, 1982, , pp. 125–148Chapter 4.

[27] J.F. McClelland, S.J. Bajic, R.W. Jones, L.M. Seaverson, Photoacoustic spectroscopy, in: F.M. Mirabella (Ed.), Modern Techniques in Applied Molecular Spectroscopy, Wiley, New York, 1998, , pp. 221–265, Chapter 6.

[28] Y.G. Yin, W.Q. Xu, S.L. Suib, C.L. O'Young, Inorg. Chem. 34 (1995) 4187.

[29] V.D. Makwana, L.J. Garces, J. Liu, J. Cai, Y.C. Son, S.L. Suib, Catal. Today 85 (2003) 225.

[30] W. Gac, A. Derylo-Marczewska, S. Pasieczna-Patkowska, N. Popivnyak, G. Zukocinski, J. Mol. Catal. A Chem. 268 (2007) 15.

[31] V. Boissel, S. Tahir, C.A. Koh, Appl. Catal. B Environ. 64 (2006) 234.

[32] M.N. Debbagh, A. Bueno-López, C.S.M. Lecea, J. Pérez-Ramírez, Appl. Catal. A Gen. 327 (2007) 66.

[33] K. Yamada, C. Pophal, K. Segawa, Micropor. Mesopor. Mater. 21 (1998) 549.

[34] T. Nobukawa, M. Yoshida, K. Okumura, K. Tomishige, K. Kunimori, J. Catal. 229 (2005) 374.